










Quantitative computed tomography predicts outcomes in idiopathic pulmonary fibrosis

Stephen M. Humphries¹  | John A. Mackintosh^{2,3}  | Helen E. Jo^{3,4} |
 Simon L. F. Walsh⁵ | Mario Silva^{6,7} | Lucio Calandriello⁸ | Sally Chapman⁹ |
 Samantha Ellis¹⁰ | Ian Glaspole^{3,11} | Nicole Goh¹²  | Christopher Grainge¹³  |
 Peter M. A. Hopkins^{2,14} | Gregory J. Keir¹⁵  | Yuben Moodley¹⁶  |
 Paul N. Reynolds¹⁷  | E. Haydn Walters¹⁸ | David Baraghoshi¹⁹ |
 Athol U. Wells^{20,21}  | David A. Lynch¹ | Tamera J. Corte^{3,4} 

¹Department of Radiology, National Jewish Health, Denver, Colorado, USA

²Department of Thoracic Medicine, The Prince Charles Hospital, Brisbane, Queensland, Australia

³NHMRC Centre of Research Excellence in Pulmonary Fibrosis, Camperdown, New South Wales, Australia

⁴Department of Respiratory Medicine, Royal Prince Alfred Hospital, Sydney, New South Wales, Australia

⁵Department of Radiology, King's College Hospital Foundation Trust, London, UK

⁶Section of "Scienze Radiologiche", Department of Medicine and Surgery (DiMeC), University of Parma, Parma, Italy

⁷Department of Radiology, University of Massachusetts Medical School, UMass Memorial Health Care, Worcester, Massachusetts, USA

⁸Dipartimento di Diagnostica per immagini, Radioterapia, Oncologia ed Ematologia, Fondazione Policlinico Universitario A. Gemelli, IRCCS, Rome, Italy

⁹Respiratory Consultants, Adelaide, South Australia, Australia

¹⁰Department of Radiology, Alfred Health, Melbourne, Victoria, Australia

¹¹Department of Allergy and Respiratory Medicine, Alfred Hospital, Melbourne, Victoria, Australia

¹²Respiratory and Sleep Medicine, Austin Hospital, Melbourne, Victoria, Australia

¹³Department of Respiratory Medicine, John Hunter Hospital, Newcastle, New South Wales, Australia

¹⁴Faculty of Medicine, The University of Queensland, Brisbane, Queensland, Australia

¹⁵Department of Respiratory Medicine, Princess Alexandra Hospital, Brisbane, Queensland, Australia

¹⁶School of Medicine & Pharmacology, University of Western Australia, Perth, Western Australia, Australia

¹⁷Department of Thoracic Medicine, Royal Adelaide Hospital, Adelaide, South Australia, Australia

¹⁸Department of Medicine, University of Tasmania, Hobart, Tasmania, Australia

¹⁹Division of Biostatistics, National Jewish Health, Denver, Colorado, USA

²⁰Royal Brompton and Harefield NHS Foundation Trust, London, UK

²¹National Heart and Lung Institute, Imperial College London, London, UK

Correspondence

John A. Mackintosh

Email: john.mackintosh@health.qld.gov.au

Funding information

National Health and Medical Research Council; Bristol-Myers Squibb Australia; Galapagos; Roche Products Pty. Limited;

Abstract

Background and objective: Prediction of disease course in patients with progressive pulmonary fibrosis remains challenging. The purpose of this study was to assess the prognostic value of lung fibrosis extent quantified at computed tomography (CT) using data-driven texture analysis (DTA) in a large cohort of well-characterized patients with idiopathic pulmonary fibrosis (IPF) enrolled in a national registry.

This research study was previously presented at the Annual Congress of the American Thoracic Society (ATS) 2020.

This is an open access article under the terms of the [Creative Commons Attribution-NonCommercial-NoDerivs](https://creativecommons.org/licenses/by-nc-nd/4.0/) License, which permits use and distribution in any medium, provided the original work is properly cited, the use is non-commercial and no modifications or adaptations are made.

© 2022 The Authors. *Respirology* published by John Wiley & Sons Australia, Ltd on behalf of Asian Pacific Society of Respiriology.

Boehringer Ingelheim;
Lung Foundation Australia

Associate Editor: Elisabetta A. Renzoni;
Senior Editor: Lutz Beckert

Methods: This retrospective analysis included participants in the Australian IPF Registry with available CT between 2007 and 2016. CT scans were analysed using the DTA method to quantify the extent of lung fibrosis. Demographics, longitudinal pulmonary function and quantitative CT metrics were compared using descriptive statistics. Linear mixed models, and Cox analyses adjusted for age, gender, BMI, smoking history and treatment with anti-fibrotics were performed to assess the relationships between baseline DTA, pulmonary function metrics and outcomes.

Results: CT scans of 393 participants were analysed, 221 of which had available pulmonary function testing obtained within 90 days of CT. Linear mixed-effect modelling showed that baseline DTA score was significantly associated with annual rate of decline in forced vital capacity and diffusing capacity of carbon monoxide. In multivariable Cox proportional hazard models, greater extent of lung fibrosis was associated with poorer transplant-free survival (hazard ratio [HR] 1.20, $p < 0.0001$) and progression-free survival (HR 1.14, $p < 0.0001$).

Conclusion: In a multi-centre observational registry of patients with IPF, the extent of fibrotic abnormality on baseline CT quantified using DTA is associated with outcomes independent of pulmonary function.

KEYWORDS

data-driven texture analysis, idiopathic pulmonary fibrosis, pulmonary function, quantitative computed tomography

INTRODUCTION

Idiopathic pulmonary fibrosis (IPF) is a progressive fibrosing interstitial lung disease (ILD) with a uniformly poor prognosis.^{1,2} Data from the recent INBUILD study, which enrolled patients with a progressive fibrotic ILD other than IPF, showed that individuals in the placebo arm had a similar rate of forced vital capacity (FVC) decline as untreated IPF.³ There is an urgent need for accurate and reproducible measures of disease behaviour for prognostication in patients with progressive pulmonary fibrosis of all aetiologies. Now that treatments are available to slow progression, it is critical to identify those with early disease who are most likely to progress.

Computed tomography (CT) plays an essential role in the evaluation of patients with ILD. However, visual assessment of disease extent, the current standard, is hampered by interobserver variation. This has motivated research into computer techniques for objective assessment of CT, which have recently shown promise in pulmonary fibrosis.⁴⁻⁶ One such technique, called data-driven texture analysis (DTA), employs deep learning methods and is capable of automatic detection and quantification of lung fibrosis on CT.⁷ Our prior work using data from IPF treatment trials has shown that the extent of fibrosis measured by DTA is associated with reduced lung function at baseline and that an increase in the DTA score on sequential CT scans is associated with physiologic decline.⁸

The purpose of this study was to evaluate the prognostic value of DTA in the large Australian Idiopathic Pulmonary Fibrosis Registry (AIPFR).^{9,10} We hypothesized that quantitative CT using a deep learning approach can stratify disease severity in patients with IPF.

SUMMARY AT A GLANCE

The extent of pulmonary fibrosis, measured objectively at baseline computed tomography using a deep learning algorithm, is associated with disease progression and mortality, independent of pulmonary function.

METHODS

Study participants

Detailed methodology on recruitment and data collection in the AIPFR has been previously published.^{2,10} The AIPFR is a multi-centre, prospective, observational registry of IPF patients across Australia. All participants of the AIPFR have a clinical diagnosis of IPF through their primary treating clinician. Participants have subsequently undergone centralized multi-disciplinary meeting (MDM) re-evaluation for the diagnosis of IPF.¹¹ We have previously demonstrated that patients behaved identically whether they met the guideline criteria for an IPF diagnosis,² and as such, we included all participants in this analysis irrespective of the diagnosis obtained after centralized MDM review. Baseline and longitudinal data were collected for the duration of a participant's enrolment.

Quantitative CT

CTs were reviewed visually to eliminate studies with quality problems such as severe patient motion, incomplete depiction of the lungs or use of intravenous contrast. Inspiratory

CT series with slice thickness ≤ 1.25 mm and spacing ≤ 20.0 mm were selected for quantitative analysis. Lung fibrosis quantification on CT images was performed using DTA, a deep learning technique consisting of convolutional neural network (CNN) algorithms trained previously using normal and abnormal scans.^{7,12} An initial CNN segments the lungs and an additional CNN classifies local image regions on axial sections as either normal or fibrotic, with the fibrotic category trained using image regions labelled by a radiologist as reticular abnormality, honeycombing or traction bronchiectasis. Subject-level CT fibrosis scores were computed as the percentage of lung pixels classified as fibrotic. In addition to DTA, histogram-based metrics were calculated using the automatically generated lung segmentation masks. These metrics included mean lung attenuation (MLA), and skewness and kurtosis of lung attenuation histograms, often referred to collectively as CT lung densitometry. To assess the effect of axial image spacing on DTA score, non-contiguous spacing was simulated by sampling axial slices at 10 mm intervals from 171 CT series with thin, contiguous images. Bland–Altman analysis was performed to compare DTA scores computed from the original volumetric CT to DTA scores computed using only sections at 10 mm intervals. Additionally, semi-quantitative visual scoring of total extent of fibrosis was performed by two radiologists (MS and LC; 10 and 13 years of experience, respectively) independent and blinded to quantitative CT results, details of which are provided in Appendix S1 in the Supporting Information.

Statistical analysis

Agreement between semi-quantitative extent of lung fibrosis scores assigned by the radiologists was evaluated using intra-class correlation coefficient (ICC). Univariate comparisons of CT-derived metrics and physiology (FVC, diffusing capacity of carbon monoxide [DLCO] and the composite physiologic index [CPI]) were calculated using Spearman's rank correlation. Kaplan–Meier plots were used to visualize transplant- and progression-free survival by groups defined by quartiles of DTA fibrosis score.

Linear mixed-effects models were fit to assess annual change in FVC and DLCO. For both parameters, separate models were fit using % predicted and raw values. All models contained variables for baseline DTA, time in years and a baseline DTA by time interaction term. Models for raw values of FVC and DLCO were adjusted by baseline age, sex, height and centred BMI. To assess DTA's contribution to assessing annual change in FVC and DLCO in the presence of baseline outcome values, models were fit utilizing baseline FVC or DLCO as covariates in addition to all pairwise interactions between baseline FVC or DLCO, baseline DTA and time. Between-subject variation was accounted for by inclusion of a random intercept for subject. Serial correlation within subjects was accounted for by specifying a spatial power covariance structure. Subjects were excluded if baseline PFT was not within 90 days of CT acquisition. DTA

TABLE 1 Demographic, CT and lung function data

No. of patients (males, females)	393 (268, 125)
Age at the time of CT, median (IQR), years	69.6 (11.0)
BMI, median (IQR)	28.2 (5.3)
Anti-fibrotic therapy, no. (%)	131 (33.3%)
Prior to CT	32 (8.1%)
After CT	99 (25.2%)
Smoking status, no. (%)	
Never	114 (29.0%)
Ever	253 (64.4%)
Current	8 (2.0%)
Missing	18 (4.5%)
Lung transplant, no. (%)	38 (9.7%)
Deceased, no. (%)	226 (57.5%)
Follow-up period, median (IQR), years	2.7 (3.3)
Contiguous CT (axial spacing ≤ 1.25 mm), no. (%)	173 (44%)
Non-contiguous CT, no. (%)	220 (66%)
Semi-quantitative CT score (%), median (IQR)	30.4 (23.3)
DTA (%), median (IQR)	31.9 (23.7)
Lung function ^a , median (IQR)	
FVC, percentage predicted, $n = 245$	79.3 (27.9)
DLCO, percentage predicted, $n = 227$	47.3 (20.9)
CPI, $n = 221$	46.0 (17.7)
Number of PFTs available, median (IQR)	5 (6)
Interval between PFTs, mean (IQR), weeks	36 (22)
GAP ^a , median (IQR), $n = 221$	4.0 (2.0)

Abbreviations: CPI, composite physiologic index; CT, computed tomography; DLCO, diffusing capacity of carbon monoxide; DTA, lung fibrosis extent quantified using data-driven texture analysis; FVC, forced vital capacity; GAP, Gender Age Physiology index; IQR, inter-quartile range; PFT, pulmonary function tests.

^aIn subjects with lung function results within 90 days of CT.

was categorized by quartiles, and annual changes for each outcome were estimated for each DTA quartile.

Multivariable Cox analysis adjusted for age, gender, BMI, smoking history, anti-fibrotic therapy and baseline lung function was performed to assess the relationships between baseline variables and risk of mortality. Progression-free survival was defined as the time from baseline HRCT to an FVC decline of $\geq 10\%$, DLCO decline $\geq 15\%$, transplant or death.

Statistical analyses were performed using R (version 3.6.0) and SAS (version 9.4). A p -value of <0.05 was considered significant.

RESULTS

The study population is summarized in Table 1. There were 393 patients in the cohort (268 men [68%] and 125 women [32%]). Participant selection is shown in Figure 1. Median age at the time of baseline CT was 69.6 years (inter-quartile range [IQR] 8.5 years). Median follow-up period was

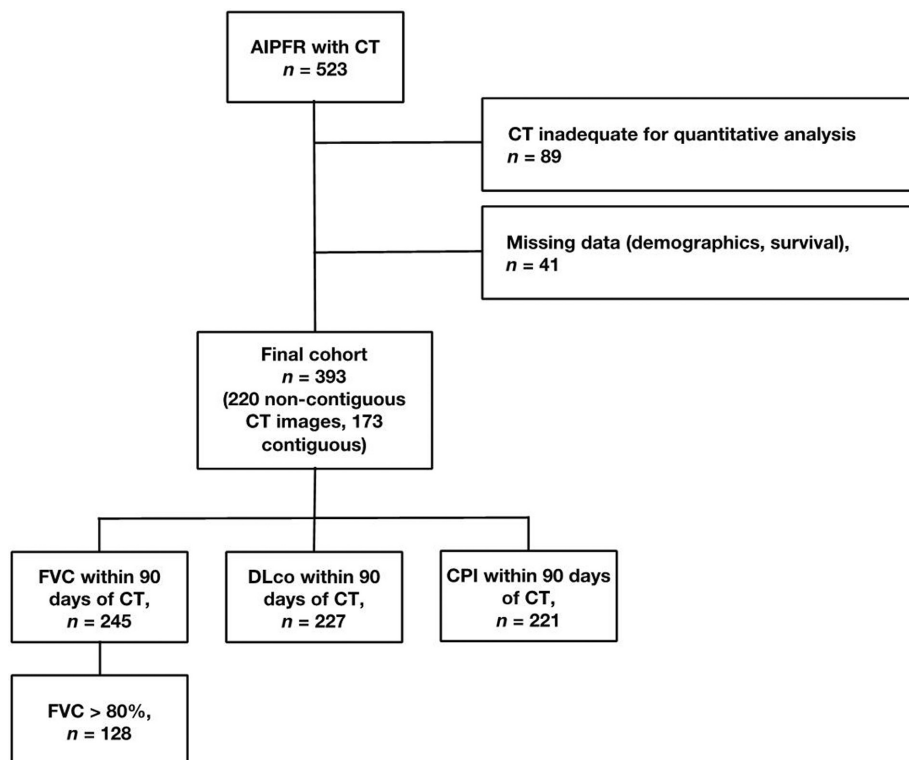


FIGURE 1 CONSORT diagram describing the study population.

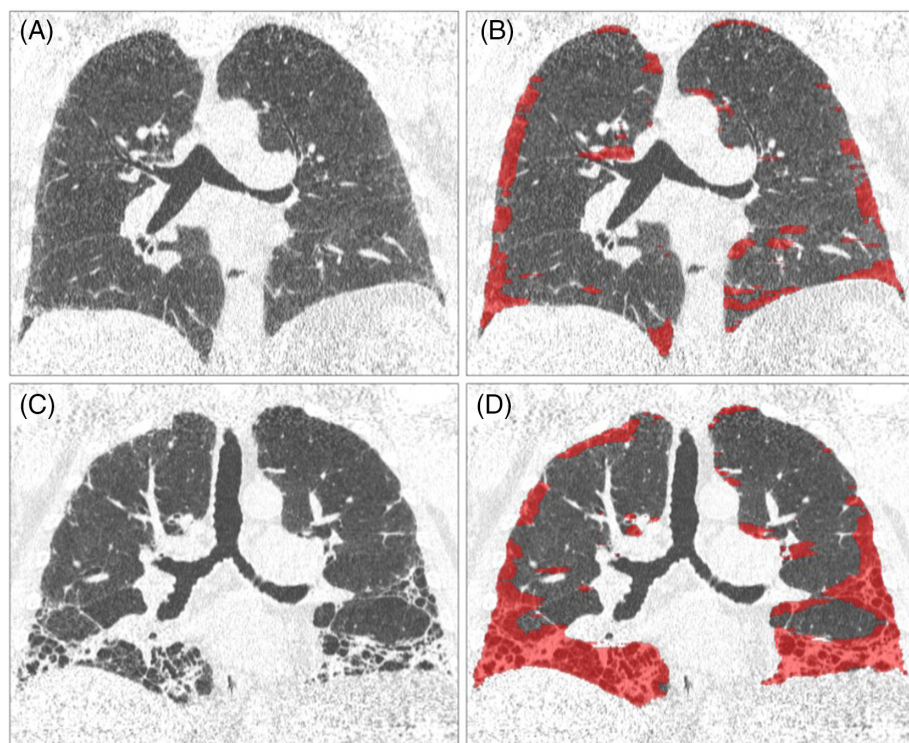


FIGURE 2 Data-driven texture analysis (DTA) enables detection, visualization and quantification of lung fibrosis. Coronal reconstructions from non-contrast, inspiratory volumetric computed tomography (CT). (A) Baseline CT from study participant with baseline forced vital capacity (FVC) 2.8 L (120.3% predicted), diffusing capacity of carbon monoxide (DLCO) 13.32 (68.7% predicted), composite physiologic index (CPI) 20.66 and DTA fibrosis score 13.93%. (B) DTA classifications in red. The patient did not progress in the 12 months following CT and remained alive without lung transplant at 3 years 2 months. (C) Baseline CT from study participant with baseline FVC 2.6 L (82.7% predicted), DLCO 8.7 (38.5% predicted), CPI 51.55 and DTA fibrosis score 48.4%. (D) DTA classifications in red. This patient died 10.5 months after CT.

2.7 years. One hundred and twenty-eight patients (32.6%) had FVC% predicted \geq 80% obtained within 90 days of baseline CT. Median DTA score was 31.9 (IQR 23.7) in the full cohort and 25.0 (IQR 20.2) in those with preserved FVC (Table S1 in the Supporting Information). Volumetric CT was available for 173 patients and 220 had imaging with

non-contiguous axial sections. Baseline CTs were obtained between 2007 and 2016. ICC comparing semi-quantitative extent scores assigned by the two radiologists was 0.62 (95% CI 0.56, 0.68). Additional details on cohort selection and CT technical parameters are available in Table S2 in the Supporting Information.

TABLE 2 Univariate associations (Spearman’s rho) between CT-derived metrics and baseline lung function (within 90 days of CT)

	Semi-quantitative CT score	DTA	MLA	Skewness	Kurtosis
FVC, percentage predicted, <i>n</i> = 245	−0.38	−0.52	−0.60	0.55	0.58
DLCO, percentage predicted, <i>n</i> = 227	−0.41	−0.58	−0.46	0.49	0.54
CPI, <i>n</i> = 221	0.46	0.63	0.56	−0.56	−0.61
Semi-quantitative CT score	-	0.71	0.62	−0.64	−0.67

Note: *p* < 0.0001 for all comparisons.

Abbreviations: CPI, composite physiologic index; CT, computed tomography; DLCO, diffusing capacity of carbon monoxide; DTA, lung fibrosis extent quantified using data-driven texture analysis; FVC, forced vital capacity; MLA, mean lung attenuation.

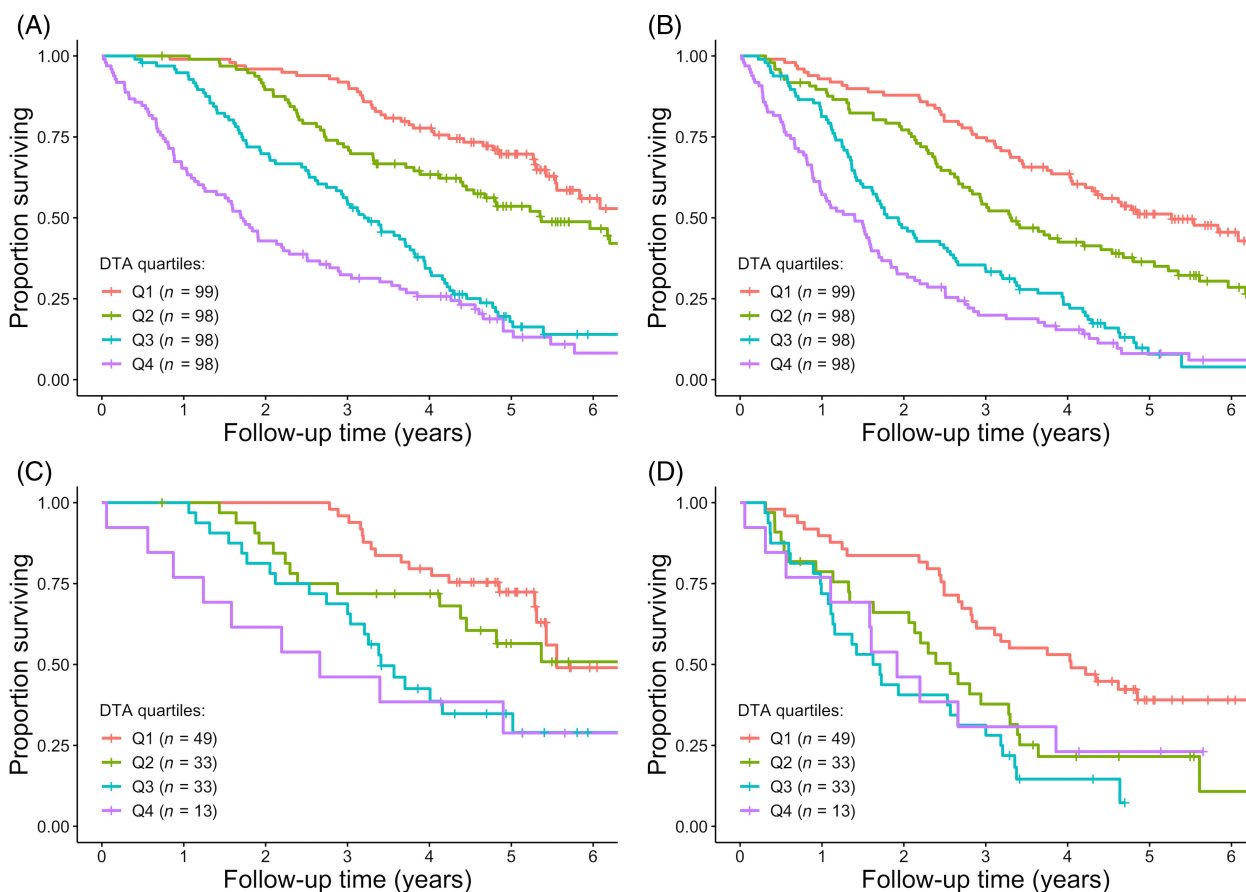


FIGURE 3 Kaplan–Meier plots showing (A) transplant-free and (B) progression-free survival by quartiles of baseline data-driven texture analysis (DTA) fibrosis score at baseline computed tomography (CT). Log-rank *p* < 0.0001 for both plots. DTA quartile ranges are: Q1 <21.2, Q2 21.3–31.9, Q3 32.1–44.9 and Q4 >45.1. Kaplan–Meier plots showing (C) transplant-free and (D) progression-free survival by quartiles of baseline DTA fibrosis score on baseline CT in patients with forced vital capacity percentage predicted ≥80% within 90 days of CT.

Figure 2 shows representative CT images and quantitative analysis results in two study participants with differing extents of lung fibrosis.

Bland–Altman analysis (Figure S1 in the Supporting Information) showed that DTA score computed from 171 CT studies with simulated 10.0 mm axial slice spacing was similar to DTA score computed using thin, contiguous axial images (mean difference in DTA was −0.035%, limits of agreement were −0.84 and 0.77).

In participants with PFT obtained within 90 days of CT (Table 2), all CT-derived metrics were moderately correlated

with FVC, DLCO and CPI (*p* < 0.0001 in all comparisons). Semi-quantitative visual extent score was moderately associated with PFTs, DTA score (Figure S2 in the Supporting Information) and histogram-based quantitative CT metrics (*p* < 0.0001).

Figure 3 shows Kaplan–Meier plots of transplant- and progression-free survival in the full cohort separated into groups defined by quartiles of DTA score (*p* < 0.0001). Limiting the analysis to the subset of participants with preserved FVC (Figure 3C,D), these thresholds in DTA score still stratified the population into groups with different risk (*p* < 0.0001).

TABLE 3 Linear mixed model estimates of annual change in FVC and DLCO by baseline DTA fibrosis score quartiles

	FVC			DLCO				
	% predicted	Litres		% predicted	ml/min/mm Hg			
DTA	Change (95% CI)	<i>p</i> -value	Change (95% CI)	<i>p</i> -value	Change (95% CI)	<i>p</i> -value	Change (95% CI)	<i>p</i> -value
Q1: (1.1–21.2)	–2.30 (–3.24, –1.37)	^a	–0.09 (–0.12, –0.07)	^a	–1.87 (–2.46, –1.27)	^a	–0.51 (–0.65, –0.36)	^a
Q2: (21.3–31.9)	–3.47 (–4.39, –2.55)	^a	–0.13 (–0.16, –0.10)	^a	–3.64 (–4.15, –3.12)	^a	–0.86 (–0.99, –0.73)	^a
Q3: (32.1–44.9)	–4.34 (–5.57, –3.10)	^a	–0.14 (–0.18, –0.11)	^a	–4.94 (–5.71, –4.17)	^a	–1.19 (–1.38, –0.99)	^a
Q4: (45.1–94.2)	–1.74 (–2.87, –0.60)	0.0027	–0.07 (–0.11, –0.04)	^a	–2.86 (–3.57, –2.14)	^a	–0.6 (–0.77, –0.42)	^a

Note: Models were fit using cases with baseline PFT within 90 days of CT acquisition.

Abbreviations: CT, computed tomography; DLCO, diffusing capacity of carbon monoxide; DTA, lung fibrosis extent quantified using data-driven texture analysis; FVC, forced vital capacity; PFT, pulmonary function tests.

^a*p* < 0.0001 unless otherwise noted.

TABLE 4 Cox proportional hazards models of transplant-free survival and progression-free survival

Variable	Per unit	Transplant-free survival			Progression-free survival		
		HR	95% CI	<i>p</i> -value	HR	95% CI	<i>p</i> -value
Model 1		Concordance 0.72			Concordance 0.62		
FVC % predicted	10%	0.91	0.81, 1.01	0.08	0.96	0.88, 1.06	0.43
DLCO % predicted	10%	0.70	0.60, 0.81	<0.0001	0.89	0.79, 0.99	0.034
Model 2		Concordance 0.72			Concordance 0.62		
CPI	10 units	1.68	1.43, 1.96	<0.0001	1.21	1.07, 1.37	0.002
Model 3		Concordance 0.73			Concordance 0.66		
DTA	5	1.20	1.14, 1.26	<0.0001	1.14	1.08, 1.19	<0.0001
Model 4		Concordance 0.67			Concordance 0.61		
Semi-quantitative	5	1.12	1.06, 1.18	<0.0001	1.08	1.03, 1.13	<0.0001
Model 5		Concordance 0.75			Concordance 0.66		
CPI	10 units	1.46	1.21, 1.75	<0.0001	1.05	0.91, 1.21	0.48
DTA	5	1.11	1.04, 1.19	0.001	1.13	1.06, 1.19	<0.0001

Note: Base models were adjusted for age, sex, BMI, smoking and treatment with anti-fibrotics. Models were fit using cases with PFTs available within 90 days of CT (*n* = 221). Of these, 136 died or underwent transplantation and 177 progressed or died in the follow-up period.

Abbreviations: CPI, composite physiologic index; CT, computed tomography; DLCO, diffusing capacity of carbon monoxide; DTA, lung fibrosis extent quantified using data-driven texture analysis; FVC, forced vital capacity; HR, hazard ratio; PFT, pulmonary function tests.

Table 3 shows linear mixed model estimates of annual mean change in FVC and DLCO by baseline DTA quartile. In general, the annual rate of physiologic decline increased with increasing DTA quartile, excluding the fourth quartile, which also showed greatest mortality risk and lower baseline pulmonary function on average (Table S2 in the Supporting Information). For both FVC and DLCO, models with baseline outcome, time and baseline outcome by time interactions were compared to models that included baseline DTA and all pairwise interactions between baseline outcome, baseline DTA and time using Akaike Information Criterion (AIC) and likelihood ratio tests. For all outcomes, models which included baseline DTA had lower AIC and significantly better fit (*p* < 0.0001), suggesting that DTA provides information beyond baseline lung function that is useful in predicting subsequent physiologic progression.

Univariate predictors of transplant- and progression-free survival are shown in Tables S4 and S5 in the Supporting Information. Results of multivariable Cox proportional

hazard models of transplant- and progression-free survival are shown in Table 4. Base models were adjusted for age, gender, BMI, smoking history and anti-fibrotic therapy. DTA was a predictor of transplant-free (model 3, hazard ratio [HR] of 1.20, 95% CI [1.14, 1.26] for each 5 unit increase in DTA, *p* < 0.0001) and progression-free survival (model 3, HR of 1.14, 95% CI [1.08, 1.19] for each 5 unit increase in DTA, *p* < 0.0001). DTA remained an independent predictor of transplant- and progression-free survival in the portion of the study cohort with FVC % predicted \geq 80% (Table 5).

DISCUSSION

Our study demonstrated, in a national registry of patients with IPF, that quantitative CT provides a direct assessment of morphologic extent of lung fibrosis that is clinically meaningful. Greater baseline DTA scores were significantly

TABLE 5 Cox proportional hazard models of transplant-free survival and progression-free survival in participants with preserved FVC

Variable	Transplant-free survival			Progression-free survival			
	HR	95% CI	p-value	HR	95% CI	p-value	
Model 1	Concordance 0.74			Concordance 0.64			
FVC % predicted	10	0.93	0.76, 1.14	0.50	1.06	0.91, 1.24	0.43
DLCO % predicted	10	0.64	0.52, 0.78	<0.001	0.82	0.70, 0.96	0.01
Model 2	Concordance 0.74			Concordance 0.61			
CPI	10 units	2.0	1.47, 2.72	<0.001	1.22	0.97, 1.53	0.09
Model 3	Concordance 0.73			Concordance 0.65			
DTA	5	1.32	1.18, 1.48	<0.001	1.16	1.07, 1.26	<0.001
Model 4	Concordance 0.69			Concordance 0.63			
Semi-quantitative	5	1.18	1.09, 1.28	<0.001	1.12	1.04, 1.20	0.002
Model 5	Concordance 0.77			Concordance 0.66			
CPI	10 units	1.76	1.26, 2.47	0.001	1.10	0.87, 1.39	0.42
DTA	5	1.28	1.14, 1.45	<0.0001	1.16	1.07, 1.26	0.0004

Note: Base models were adjusted for age, sex, BMI, smoking and treatment with anti-fibrotics. Models were fit using 108 participants with all data available. Of these, 57 died or underwent transplantation and 84 progressed or died in the follow-up period.

Abbreviations: CPI, composite physiologic index; DLCO, diffusing capacity of carbon monoxide; DTA, lung fibrosis extent quantified using data-driven texture analysis; FVC, forced vital capacity; HR, hazard ratio.

associated with subsequent rate of decline in FVC and DLCO and with increased risk of mortality. The inclusion of DTA improved the prediction of disease progression in models that comprised baseline functional measures of disease severity like CPI. This extends our previous work in independent clinical trial populations where we showed that greater DTA fibrosis score on baseline CT was associated with increased risk of disease progression and all-cause hospitalization,¹³ and an increase in DTA fibrosis extent on sequential scans is associated with physiologic decline.⁸ These results in a cohort of IPF patients lend support for the evaluation of DTA in progressive pulmonary fibrosis more broadly.

The precise measurement of morphology using imaging and deep learning may provide important insight for clinical decision-making related to anti-fibrotic therapy and for design of inclusion criteria for clinical trials. There remains some variability amongst physicians as to the best timing for commencement of anti-fibrotic therapy, with some preferring a 'watch-and-wait' approach particularly in those with milder disease, and others opting to start therapy at diagnosis.¹⁴ Current predictive models do not help to stratify individual patients for disease progression. In the setting of early disease, there may be value in the discriminatory power of CT and DTA to differentiate those who are likely and less likely to progress. A greater extent of lung fibrosis using quantitative CT could support the early commencement of therapy. In the clinical trial setting, inclusion on the basis of pre-specified DTA scores might help to improve study power, particularly in the era of IPF clinical trials comprising background anti-fibrotic therapy. The ability of DTA to improve the prediction of disease progression may also assist with the timing of lung transplant evaluation and listing.

In this study, we demonstrate the capability of DTA at baseline CT to determine the risk of future disease progression in IPF. By demonstrating the ability of DTA to stratify the risk of disease progression at baseline in IPF, we provide the foundations for future evaluation in other progressive fibrosing lung diseases. Accurately defining the risk of fibrotic disease progression at baseline would enable earlier institution of anti-fibrotic therapy before irreversible progression has occurred. The radiological similarities, in particular shared usual interstitial pneumonia-like features, between IPF and other progressive fibrotic lung diseases, support the evaluation of DTA across the broader landscape of fibrotic ILD.

This study shows that fibrosis extent scores calculated from non-contiguous images are comparable to those calculated using volumetric imaging in a population with clinical diagnosis of IPF. While volumetric imaging captures a more complete representation of the lungs, and is generally recommended for the evaluation of IPF,¹¹ such radiologic examinations are sometimes not performed in clinical practice. The finding that DTA was reliable in a real-world, retrospective cohort across varying CT technical parameters further strengthens its generalizability.

Quantitative CT using lung densitometry has been applied to study IPF for some time.¹⁵⁻¹⁷ Metrics such as MLA and skewness and kurtosis of lung pixel histograms consistently correlate with physiology and are appealing in that they are relatively easy to understand and implement. These measurements summarize the frequency distribution of CT attenuation values over the lung volume. While they are affected somewhat by the presence of diffuse abnormalities, they do not specifically detect and localize regions of fibrosis. Classification of abnormal areas on CT is a pattern recognition problem that is better addressed by machine learning methods that capitalize on diverse features

including texture, a quality of images formed by structure in the spatial arrangement and intensity of image pixels. As we have shown previously,⁷ the present study confirms that the extent of lung fibrosis quantified using a machine learning method is more strongly associated with physiology and outcomes than are metrics based on lung densitometry, or semi-quantitative visual scores.

A number of other methods that leverage machine learning principles for assessment of IPF on CT have been successful.^{4,18–20} Most prior work relies on engineered image features, meaning that features used as input to classification algorithms were designed manually, often using combinations of statistical calculations and heuristics. Jacob et al. showed that the CALIPER system, whose classification algorithms are based on pixel intensity histograms in small volumes of interest in the lungs, provides indices of severity that are more prognostically accurate in IPF than visual assessment.²¹ Kim and colleagues showed that a classifier based on statistical image texture metrics can produce scores for the extent of fibrotic ILD that are associated with baseline disease extent and are also a sensitive measure of change over time.¹⁸ DTA, on the other hand, is based on a deep learning approach where CNNs learn optimal features for discriminating lung fibrosis based on examples labelled by expert radiologists.

This study has limitations, largely related to the real-world nature of the registry, selection biases present in this cohort and mixed CT technical characteristics that are unavoidable in retrospective analysis of scans acquired without a standardized protocol. The statistical associations that were observed despite these variations suggest that a CNN approach like DTA is versatile and can accommodate varying CT technical characteristics to some degree. That said, more consistent imaging parameters would likely improve precision in a similar project and future prospective studies would benefit from standardized CT acquisition and reconstruction procedures in order to minimize variation. Results would also be bolstered by comparison with an independent cohort.

In conclusion, these analyses in the AIPFR show important associations between morphologic extent of pulmonary fibrosis, measured objectively on CT using a deep learning algorithm, and outcomes, independent of pulmonary function. The results from this IPF cohort support further studies to evaluate the application of DTA in other forms of progressive pulmonary fibrosis.

AUTHOR CONTRIBUTION

Stephen M. Humphries: Conceptualization (lead); data curation (lead); formal analysis (lead); investigation (lead); methodology (lead); resources (lead); software (lead); writing – original draft (lead); writing – review and editing (lead). **Helen E. Jo:** Data curation (equal); writing – review and editing (equal). **Simon L. F. Walsh:** Conceptualization (equal); methodology (equal); writing – review and editing (equal). **Mario Silva:** Methodology (equal); writing – review and editing (equal). **Lucio Calandriello:**

Methodology (equal); writing – review and editing (equal). **Sally Chapman:** Data curation (equal); writing – review and editing (equal). **Samantha Ellis:** Data curation (equal); writing – review and editing (equal). **Ian Glaspole:** Data curation (equal); writing – review and editing (equal). **Nicole Goh:** Data curation (equal); writing – review and editing (equal). **Christopher Grainge:** Data curation (equal); writing – review and editing (equal). **Peter M. A. Hopkins:** Data curation (equal); writing – review and editing (equal). **Gregory J. Keir:** Data curation (equal); writing – review and editing (equal). **Yuben Moodley:** Data curation (equal); writing – review and editing (equal). **Paul N. Reynolds:** Data curation (equal); writing – review and editing (equal). **E. Haydn Walters:** Data curation (equal); writing – review and editing (equal). **David Baraghoshi:** Formal analysis (supporting); methodology (supporting); writing – original draft (supporting). **Athol U. Wells:** Data curation (equal); methodology (equal); writing – review and editing (equal). **David A. Lynch:** Conceptualization (equal); data curation (equal); investigation (equal); methodology (equal); supervision (equal); writing – original draft (equal); writing – review and editing (equal). **Tamera J. Corte:** Conceptualization (equal); data curation (equal); methodology (equal); resources (equal); supervision (equal); writing – original draft (equal); writing – review and editing (equal). **John A. Mackintosh:** Conceptualization (equal); data curation (equal); writing – original draft (supporting); writing – review and editing (equal).

ACKNOWLEDGEMENTS

Research funding: The study was supported by Australian IPF Registry and funded by the NHMRC Centre of Research Excellence in Pulmonary Fibrosis (which in turn is supported by Lung Foundation Australia and industry sponsors including Boehringer Ingelheim, Roche Products Pty. Limited, Galapagos and Bristol-Myers Squibb Australia). Information on the Australian IPF Registry is available at: <https://lungfoundation.com.au/research/our-research/australian-ipf-registry/> Open access publishing facilitated by The University of Queensland, as part of the Wiley - The University of Queensland agreement via the Council of Australian University Librarians. Open access publishing facilitated by The University of Queensland, as part of the Wiley - The University of Queensland agreement via the Council of Australian University Librarians.

CONFLICTS OF INTEREST

The NHMRC Centre of Research Excellence in Pulmonary Fibrosis is supported by Lung Foundation Australia and industry sponsors including Boehringer Ingelheim, Roche Products Pty. Limited, Galapagos and Bristol-Myers Squibb Australia.

NG reports personal fees from AstraZeneca, Roche and Boehringer Ingelheim, and non-financial support from Air Liquide, all outside the submitted work. TJC reports grants and personal fees from Boehringer Ingelheim, Roche and

Bristol Meiers Squibb; personal fees from Promedior and Ad Alta; and grants from Avalyn Pharma and Biogen, all outside the submitted work.

DATA AVAILABILITY STATEMENT


The data that support the findings of this study are available on request from the corresponding author. The data are not publicly available due to privacy or ethical restrictions.

HUMAN ETHICS APPROVAL DECLARATION


Ethical approval was granted by the Sydney Local Health District ethics committee (protocol number X14-0264). All participants of this study have provided written consent to be enrolled in the Australian IPF Registry, which includes access to their CT for research purposes.

ORCID

Stephen M. Humphries  <https://orcid.org/0000-0002-5113-4530>

John A. Mackintosh  <https://orcid.org/0000-0002-5254-4144>

Nicole Goh  <https://orcid.org/0000-0003-2065-4346>

Christopher Grainge  <https://orcid.org/0000-0002-6565-9928>

Gregory J. Keir  <https://orcid.org/0000-0001-9979-8726>

Yuben Moodley  <https://orcid.org/0000-0002-0777-1196>

Paul N. Reynolds  <https://orcid.org/0000-0002-2273-1774>

Athol U. Wells  <https://orcid.org/0000-0003-2108-6248>

Tamera J. Corte  <https://orcid.org/0000-0002-7096-9365>

REFERENCES

- Raghu G, Remy-Jardin M, Myers JL, Richeldi L, Ryerson CJ, Lederer DJ, et al. Diagnosis of idiopathic pulmonary fibrosis. An official ATS/ERS/JRS/ALAT clinical practice guideline. *Am J Respir Crit Care Med.* 2018;198(5):e44–68.
- Jo HE, Glaspole I, Goh N, Hopkins PM, Moodley Y, Reynolds PN, et al. Implications of the diagnostic criteria of idiopathic pulmonary fibrosis in clinical practice: analysis from the Australian Idiopathic Pulmonary Fibrosis Registry. *Respirology.* 2019;24(4):361–8.
- Flaherty KR, Wells AU, Cottin V, Devaraj A, Walsh SL, Inoue Y, et al. Nintedanib in progressive fibrosing interstitial lung diseases. *N Engl J Med.* 2019;381(18):1718–27.
- Wu X, Kim GH, Salisbury ML, Barber D, Bartholmai BJ, Brown KK, et al. Computed tomographic biomarkers in idiopathic pulmonary fibrosis: the future of quantitative analysis. *Am J Respir Crit Care Med.* 2019;199:12–21.
- Walsh SL, Humphries SM, Wells AU, Brown KK. Imaging research in fibrotic lung disease; applying deep learning to unsolved problems. *Lancet Respir Med.* 2020;8:1144–53.
- Walsh SL, Calandriello L, Silva M, Sverzellati N. Deep learning for classifying fibrotic lung disease on high-resolution computed tomography: a case-cohort study. *Lancet Respir Med.* 2018;6:837–45.
- Humphries SM, Yagihashi K, Huckleberry J, Rho BH, Schroeder JD, Strand M, et al. Idiopathic pulmonary fibrosis: data-driven textural analysis of extent of fibrosis at baseline and 15-month follow-up. *Radiology.* 2017;285:270–8.
- Humphries S, Swigris J, Brown K, Strand M, Gong Q, Sundry J, et al. Quantitative high-resolution computed tomography fibrosis score:

performance characteristics in idiopathic pulmonary fibrosis. *Eur Respir J.* 2018;52(3):1801384.

- Moodley Y, Goh N, Glaspole I, Macansh S, Walters EH, Chapman S, et al. Australian Idiopathic Pulmonary Fibrosis Registry: vital lessons from a national prospective collaborative project. *Respirology.* 2014;19(7):1088–91.
- Jo HE, Glaspole I, Grainge C, Goh N, Hopkins PM, Moodley Y, et al. Baseline characteristics of idiopathic pulmonary fibrosis: analysis from the Australian Idiopathic Pulmonary Fibrosis Registry. *Eur Respir J.* 2017;49(2):1601592.
- Raghu G, Collard HR, Egan JJ, Martinez FJ, Behr J, Brown KK, et al. An official ATS/ERS/JRS/ALAT statement: idiopathic pulmonary fibrosis: evidence-based guidelines for diagnosis and management. *Am J Respir Crit Care Med.* 2011;183(6):788–824.
- Mathai SK, Humphries S, Kropski JA, Blackwell TS, Powers J, Walts AD, et al. MUC5B variant is associated with visually and quantitatively detected preclinical pulmonary fibrosis. *Thorax.* 2019;74(12):1131–9.
- Raghu G, Ley B, Brown KK, Cottin V, Gibson KF, Kaner RJ, et al. Risk factors for disease progression in idiopathic pulmonary fibrosis. *Thorax.* 2020;75(1):78–80.
- Jo HE, Glaspole I, Moodley Y, Chapman S, Ellis S, Goh N, et al. Disease progression in idiopathic pulmonary fibrosis with mild physiological impairment: analysis from the Australian IPF registry. *BMC Pulm Med.* 2018;18(1):19.
- Best AC, Lynch AM, Bozic CM, Miller D, Grunwald GK, Lynch DA. Quantitative CT indexes in idiopathic pulmonary fibrosis: relationship with physiologic impairment. *Radiology.* 2003;228(2):407–14.
- Best AC, Meng J, Lynch AM, Bozic CM, Miller D, Grunwald GK, et al. Idiopathic pulmonary fibrosis: physiologic tests, quantitative CT indexes, and CT visual scores as predictors of mortality. *Radiology.* 2008;246(3):935–40.
- Loeh B, Brylski LT, von der Beck D, Seeger W, Krauss E, Bonniaud P, et al. Lung CT densitometry in idiopathic pulmonary fibrosis for the prediction of natural course, severity, and mortality. *Chest.* 2019;155(5):972–81.
- Kim HJ, Brown MS, Chong D, Gjertson DW, Lu P, Kim HJ, et al. Comparison of the quantitative CT imaging biomarkers of idiopathic pulmonary fibrosis at baseline and early change with an interval of 7 months. *Acad Radiol.* 2015;22(1):70–80.
- Salisbury ML, Lynch DA, Van Beek EJ, Kazerooni EA, Guo J, Xia M, et al. Idiopathic pulmonary fibrosis: the association between the adaptive multiple features method and fibrosis outcomes. *Am J Respir Crit Care Med.* 2017;195(7):921–9.
- Bartholmai BJ, Raghunath S, Karwoski RA, Moua T, Rajagopalan S, Maldonado F, et al. Quantitative CT imaging of interstitial lung diseases. *J Thorac Imaging.* 2013;28(5):298–307.
- Jacob J, Bartholmai BJ, Rajagopalan S, Kokosi M, Nair A, Karwoski R, et al. Mortality prediction in idiopathic pulmonary fibrosis: evaluation of computer-based CT analysis with conventional severity measures. *Eur Respir J.* 2017;49(1):1601011.

SUPPORTING INFORMATION

Additional supporting information can be found online in the Supporting Information section at the end of this article.

How to cite this article: Humphries SM, Mackintosh JA, Jo HE, Walsh SLF, Silva M, Calandriello L, et al. Quantitative computed tomography predicts outcomes in idiopathic pulmonary fibrosis. *Respirology.* 2022;27(12):1045–53. <https://doi.org/10.1111/resp.14333>